

# Unifying Multimodal Large Language Model Capabilities and Modalities via Model Merging

**Yongxian Wei<sup>1</sup> Runxi Cheng<sup>1</sup> Weike Jin<sup>2</sup> Enneng Yang<sup>3</sup> Li Shen<sup>3</sup>  
Lu Hou<sup>2</sup> Sinan Du<sup>1</sup> Chun Yuan<sup>1</sup> Xiaochun Cao<sup>3</sup> Dacheng Tao<sup>4</sup>**

<sup>1</sup>Tsinghua University; <sup>2</sup>Huawei Noah’s Ark Lab

<sup>3</sup>Sun Yat-sen University; <sup>4</sup>Nanyang Technological University

{weiyx23, crx23}@mails.tsinghua.edu.cn; mathshenli@gmail.com  
{houlu3, jinweike}@huawei.com; yuanc@sz.tsinghua.edu.cn

## Abstract

While foundation models update slowly due to resource-intensive training requirements, domain-specific models evolve between updates. Model merging aims to combine multiple expert models into a single, more capable model, thereby reducing storage and serving costs while supporting decentralized model development. Despite its potential, previous studies have primarily focused on merging visual classification models or Large Language Models (LLMs) for code and math tasks. Multimodal Large Language Models (MLLMs), which extend the capabilities of LLMs through large-scale multimodal training, have gained traction. However, there lacks a benchmark for model merging research that clearly divides the tasks for MLLM training and evaluation. In this paper, (i) we introduce the model merging benchmark for MLLMs, which includes multiple tasks such as VQA, Geometry, Chart, OCR, and Grounding, providing both LoRA and full fine-tuning models. Moreover, we explore how model merging can combine different modalities (*e.g.*, vision-language, audio-language, and video-language models), moving toward the Omni-language model. (ii) We implement 10 model merging algorithms on the benchmark. Furthermore, we propose a novel method that removes noise from task vectors and robustly optimizes the merged vector based on a loss defined over task vector interactions, achieving an average performance gain of 2.48%. (iii) We find that model merging offers a promising way for building improved MLLMs without requiring data training. Our results also demonstrate that the complementarity among multiple modalities outperforms individual modalities. All code and checkpoints are publicly available [here](#).

## 1 Introduction

Foundation models experience slow development cycles due to resource-intensive training requirements, while domain-specific models continuously improve during interim periods [21]. Various developers release their fine-tuned models on open-source communities such as Hugging Face. Model merging [85] aims to combine multiple expert models into a unified model with multiple capabilities. This approach reduces storage and serving costs through model reuse, while supporting decentralized development by enabling independent contributors to build models that can later be merged. Despite its potential, previous studies [4, 35, 86] have primarily focused on merging visual classification models across multiple datasets to extract representations, or merging Large Language Models (LLMs) specifically for code and math tasks.

Multimodal Large Language Models (MLLMs), which extend LLMs with broader capabilities through large-scale multimodal training, have gained traction. Model merging offers a cost-effective way to

combine fine-tuned MLLMs with task-specific skills into a unified model (see Fig. 1). However, there lacks a benchmark for model merging research that clearly divides the tasks for MLLM training and evaluation. Specifically, AdaMMS [19] proposes an unsupervised hyper-parameter selection method, but can only merge two MLLMs at a time. For example, merging LLaVA-OneVision-Qwen [43] into Qwen2-VL [77] on the Qwen2 architecture. UQ-Merge [65] treats each fine-tuning dataset in LLaVA-v1.5 [48] as a separate task without categorization of MLLM capabilities, fine-tuning the base model for each dataset and using LLaVA-v1.5 as the mixture training baseline.

In this paper, we introduce a model merging benchmark for MLLMs, which includes diverse tasks such as VQA, Geometry, Chart, OCR, and Grounding. For each task, we collect comprehensive public datasets with at least 100k samples to ensure effective supervised fine-tuning, and select corresponding benchmarks to evaluate distinct capabilities. We derive an upper bound on the error between the merged model and expert models, proving that merging performance is influenced by the learning rate and iterations, which control the extent of parameter drift. Smaller parameter changes lead to easier merging. We choose two types of vision-language models: InternVL2.5 and Qwen2-VL, providing both LoRA and full fine-tuning checkpoints. Moreover, most existing MLLMs specialize in dual modalities, and incorporating new modality encoders requires re-training on new modality-text data. Generating high-quality multimodal instruction data is resource-consuming [36]. Therefore, we explore how model merging can efficiently combine different modalities (*e.g.*, vision-language, audio-language, and video-language models), moving toward the Omni-language model. This offers a data-free way to reuse and integrate modality-specific encoders into a unified LLM.

Based on our benchmark, we conduct an in-depth comparison and analysis of state-of-the-art merging methods in capability and modality merging settings. Furthermore, we propose a novel merging method that improves the task vector (*i.e.*, the parameter change between fine-tuned and base models) optimization. This method optimizes the merged model based on a loss defined over task vector interactions and applies low-rank approximations to reduce redundant noise, achieving the best results. Combining multiple MLLMs without additional data training, the merged model can even outperform expert MLLMs in their respective capabilities and mixture data training. We also find that merging methods effectively integrate inputs from multiple modalities, outperforming models trained on individual modalities, thus emphasizing the complementary nature of modal information.

In summary, our main contributions are three-fold:

- **Benchmark:** We introduce the model merging benchmark with detailed categorization of MLLM capabilities, and explore how model merging can effectively combine different modalities of MLLMs. We hope this benchmark will help the model merging community better evaluate the generalizability of their methods.
- **Methodology:** We further propose a novel merging method that effectively removes noise from task vectors and improves the robustness of merged vector optimization. Ablation studies show that it achieves an average performance gain of 2.48%.
- **Experiments:** We conduct comprehensive experiments and discussions on our benchmark. The empirical results demonstrate that model merging potentially surpasses mixture training, serving as a way for omni model alignment, while offering a scalable solution for developing MLLMs with reduced computational cost and time.

## 2 Related Work

**Model merging.** Model merging has emerged as a cost-effective approach to developing improved models by combining multiple expert models to leverage their complementary capabilities [3, 85]. These expert models typically share a common base model, with specialization achieved through fine-tuning on distinct datasets. This approach offers a flexible and modular method for post-training

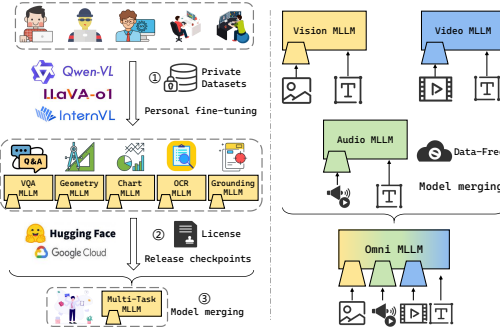


Figure 1: Unifying the **capabilities** or **modalities** of MLLMs from open-source communities via model merging, which is cost-effective.

MLLMs and facilitates the integration of new capabilities into top-performing models. Current research on model merging falls into two primary categories: static merging and dynamic merging. **Static merging** compresses multiple models into a single standard-sized model without adding additional computation or memory overhead. **Dynamic merging** (aka MoE-like methods) [32, 52, 74] requires the dynamic loading of task-specific modules based on test inputs, involving training routers or prior knowledge. The storage parameters for dynamic merging are larger.

Static merging can be further divided into data-free methods and test-time adaptation methods. **Data-free methods** merge fine-tuned models without requiring additional data. We categorize these methods into four groups: (i) Linear interpolation methods that perform arithmetic operations on task vectors [11, 26, 35, 82]; (ii) Sparsification-based methods that reduce redundancy in task vectors [31, 84, 93]; (iii) SVD-based methods that identify and exploit the low-rank features of task vectors [15, 24, 56, 70]; and (iv) Optimization-based methods that optimize task vectors via gradient descent [14, 80]. **Test-time adaptation** [17, 87, 88] assumes access to unlabeled test datasets, which can be considered a form of transductive learning.

Although test-time adaptation and dynamic merging achieve remarkable results, their practical applicability is limited due to challenges including data privacy concerns, additional storage requirements, and insufficient parallelism in merged models. Therefore, we focus on data-free static merging.

**Model merging in MLLMs.** Recently, several works have attempted model merging for MLLMs, but with different objectives. VL-merging [71] merges modality-specific pre-trained models to create modality-agnostic models, evaluating their effectiveness through fine-tuning on downstream tasks (*e.g.*, image-text retrieval and image classification). VisionFuse [12] employs task arithmetic to merge LLMs with concatenated visual encoder outputs, primarily focusing on enhancing MLLMs’ visual capabilities. DAMC [7] composes MLLMs across image, audio, video, and point cloud modalities while reducing modal interference through parameter decoupling.

Several approaches similar to ours aim to merge multiple MLLMs to improve multi-task performance. AdamMS [19] proposes an unsupervised hyperparameter selection method for model merging. However, it requires generating responses for each candidate hyperparameter, making it time-consuming and assuming test set availability during merging. Furthermore, it can only merge two models at a time. For example, merging LLaVA-OneVision-Qwen into Qwen2-VL on the Qwen2 architecture, or merging LLaVA-v1.5 into CogVLM-Chat on the LLaMA architecture. UQ-Merge [65] considers uncertainty quantification on text and vision inputs to examine MLLM prediction confidence, requiring unlabeled test sets to calculate prediction and determine merging sequence. This approach is computationally expensive as it measures uncertainty across all candidate models and repeatedly evaluates merged models to find optimal combinations. UQ-Merge treats each fine-tuning dataset in LLaVA-v1.5 [48] as a separate task without categorization of MLLM capabilities, fine-tuning the base model for each dataset and using LLaVA-v1.5 as the mixture training baseline. In contrast, our benchmark collects more comprehensive data with clearer MLLM task divisions for fine-tuning, and we propose a data-free method that requires no hyperparameter search.

### 3 Rethinking Model Merging

Model merging aims to integrate multiple fine-tuned models, all derived from a base model  $\theta_0$ , into a unified model that consolidates knowledge from diverse sources. Given  $n$  fine-tuned models denoted as  $\theta_1, \dots, \theta_n$ , the objective is to produce a single merged model  $\theta_m$  that effectively inherits the capabilities of all individual models.

#### 3.1 Merging Baselines

We categorize existing merging methods into four groups and briefly introduce each.

**Linear interpolation methods:** **Weight Averaging** [82] simply averages the weights of models fine-tuned on different tasks. **Task Arithmetic** [35] computes task vectors  $\tau_i = \theta_i - \theta_0$  for individual tasks and sums them to form a multi-task vector  $\tau_m = \sum_{i=1}^n \tau_i$ . This vector is then scaled by a coefficient  $\lambda$  and added to the base model  $\theta_0$  to obtain the merged model.

**Sparsification-based methods:** **Ties-Merging** [84] combines steps like trimming, parameter sign determination, and disjoint merging to produce a merged task vector  $\tau_m$ . The final model is defined

as  $\theta_m = \theta_0 + \lambda \tau_m$ , where  $\lambda$  is tuned using the validation set. **DARE** [93] randomly drops redundant task vectors and rescales the remaining ones to mitigate parameter interference.

**SVD-based methods:** **TSV Merging** [24] quantifies task-specific feature overlap in weight space by measuring the singular task interference of  $\tau_i$ . It then reduces task interference through decorrelation, which is mathematically formulated as an orthogonal Procrustes problem. The method seeks orthogonal matrices  $V_\perp$  and  $U_\perp$  to reconstruct the parameters of the merged model. **Iso-C** [56] proposes an isotropic merging framework that flattens the singular value spectrum of task matrices, and enhances alignment between singular components of task-specific and merged matrices.

**Optimization-based methods:** **WUDI Merging** [14] proves that task vectors  $\tau$  form an approximate linear subspace of the fine-tuning data  $x$ . This property allows the implicit utilization of training data information through task vectors alone. They define layer-wise interference between the merged vector and task vector as  $\tau_{m,l} - \tau_{i,l}$  for task  $i$  at layer  $l$ . To optimize the merged vector  $\tau_{m,l}$ , they minimize this interference  $(\tau_{m,l} - \tau_{i,l})x_i$  with respect to task input  $x_i$ . Leveraging the linear subspace relationship, they substitute the transpose of  $\tau_{i,l}$  for  $x_{i,l}$ :

$$\min_{\tau_{m,l}} \mathcal{L}_l = \sum_{i=1}^n \frac{1}{\|\tau_{i,l}\|_F^2} \|(\tau_{m,l} - \tau_{i,l})(\tau_{i,l})^\top\|_F^2. \quad (1)$$

### 3.2 Parameter Changes during Fine-tuning Matter

Model merging exhibits sensitivity to task vectors  $\tau_i$  (*i.e.*, parameter changes between fine-tuned models and the base model). Several studies [35, 45, 93] demonstrate that less intensive fine-tuning can yield superior merging performance, even when these models achieve lower accuracy on their respective tasks. In App. B, we conduct experiments on the impact of fine-tuning steps on merging performance, and observe that performance tends to rise initially and then decline. This counter-intuitive finding suggests that higher-performing expert models do not necessarily produce better merging outcomes. Fine-tuned models tend to converge around the base model in parameter space [16, 61]. When constructing our benchmark, we deliberately reduce parameter changes by lowering the learning rate while ensuring performance improvements on specific tasks. We analyze the upper bound of the loss incurred by model merging:

**Theorem 3.1.** *Let  $\theta_0 \in \mathbb{R}^d$  be the initial parameter. For each task  $i$ , after  $T$  gradient steps with constant learning rate  $\eta$ , we denote the task vector as  $\tau_i = \theta_i - \theta_0$ . Considering that most methods can be viewed as extensions of linear combinations of task vectors, let  $\tau_m = \sum_j \alpha_j \tau_j$  denote the merged vector. The loss on task  $i$  is denoted by  $\mathcal{L}_i(\Theta)$ , which is  $C_i$ -Lipschitz continuous. Assuming a constraint on the second moment of the gradient, then:*

$$\|\mathcal{L}_i(\theta_0 + \tau_m) - \mathcal{L}_i(\theta_0 + \tau_i)\| \leq \mathcal{O}(\eta T) \quad (2)$$

*This indicates that both the learning rate and iterations influence model merging results. Please refer to App. A for detailed assumptions and proofs.*

We examine the weight magnitude distribution of task vectors across our benchmark (see Fig. 2 (a-b)). Our analysis reveals that InternVL2.5, which undergoes full fine-tuning, exhibits a right-skewed distribution with parameter values concentrated around 1e-3. In contrast, Qwen2-VL, fine-tuned using LoRA, displays a multi-modal distribution with parameter values fluctuating between 1e-4 and 1e-5. Both models demonstrate distinct magnitude distribution patterns across different tasks. We also compute the normalized Frobenius norm of parameters (*i.e.*, divided by the number of parameters). As shown in Fig. 2 (c-d), the Frobenius norm varies significantly across tasks and layers, which presents challenges that we will address in our approach. The small task vector magnitudes suggest that fine-tuned models and base models exist in adjacent regions of the loss landscape with linear connectivity [83], facilitating effective model merging [63, 75].

## 4 Methodology

WUDI merging defines a loss between the merged vector  $\tau_m$  and task vectors  $\tau_i$  to learn the merged vector. Building on this foundation, we propose improved task vector optimization.

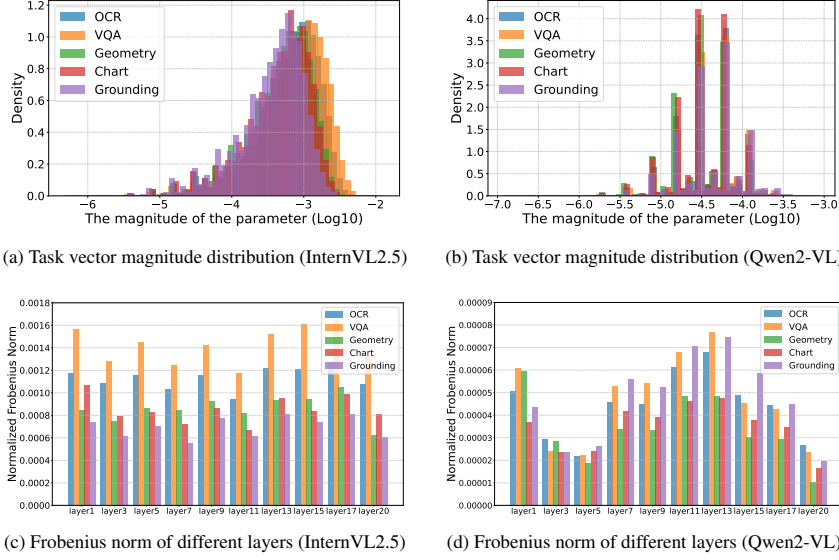


Figure 2: **Visualization of task vectors from the benchmark**, revealing the small extent of parameter changes during fine-tuning. InternVL2.5 (full fine-tuning) and Qwen2-VL (low-rank adaptation) exhibit distinct distribution patterns across different tasks.

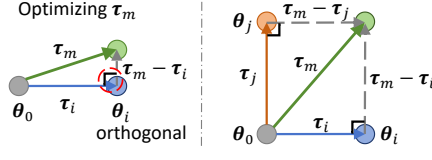


Figure 3:  $\tau_m$  tends to take shortcuts by increasing its magnitude to encourage orthogonality.

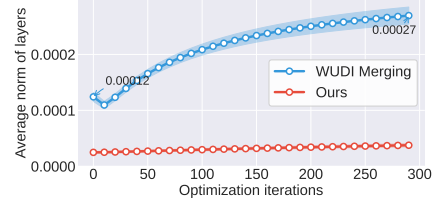


Figure 4: Frobenius norm of the merged vector changes during optimization (average by layers).

**For full fine-tuning.** Task vectors contain extreme redundancy and noise that create mutual interference, impeding effective merge vector optimization. To address this issue, we propose reducing inter-task interference through low-rank approximation. First, we calculate the average task vector  $\bar{\tau}_l = \frac{1}{n} \sum_{i=1}^n \tau_{i,l}$  and use it to center task vectors [15]. Next, we perform SVD to isolate core task-specific knowledge from noise present in the top and lower singular vectors.

$$\text{SVD}(\tau_{i,l} - \bar{\tau}_l) = U\Sigma V^\top, \text{ where } U \in \mathbb{R}^{m \times r}, \Sigma \in \mathbb{R}^{r \times r}, V \in \mathbb{R}^{n \times r}. \quad (3)$$

We then apply low-rank approximations to eliminate redundant noise, where  $U_{1:k}, \Sigma_{1:k}, V_{1:k}^\top$  represent the top- $k$  singular components. Moreover, we find that substituting  $\Sigma_{1:k} V_{1:k}^\top$  for the task vector  $\tau_{i,l}$  as the input subspace  $x_{i,l}$  allows us to discard secondary row space information, focusing only on the column feature space. Thus, we can optimize  $\tau_{m,l}$  via gradient decent on the loss:

$$\min_{\tau_{m,l}} \mathcal{L}_l = \sum_{i=1}^n \frac{1}{\|\tau_{i,l}\|_F^2} \|(\tau_{m,l} - U_{1:k} \Sigma_{1:k} V_{1:k}^\top - \bar{\tau}_l)(\Sigma_{1:k} V_{1:k}^\top)^\top\|_F^2. \quad (4)$$

By truncating singular values, we preserve critical features  $V_{1:k}^\top$ , which is similar to selecting principal components in PCA [1]. This results in more accurate input  $x_{i,l}$  estimations.

**For LoRA fine-tuning.** The inherent low-rank nature of LoRA fine-tuning presents unique optimization challenges for the merge vector. When optimizing  $\tau_{m,l}$ , gradients become effective only in directions corresponding to non-zero singular values of  $\tau_{i,l}$ , while approaching zero in other directions (null space). This constraint limits parameter update freedom, preventing  $\tau_{m,l}$  from properly exploring the parameter space. We observe that  $\tau_{m,l}$  tends to take shortcuts by increasing its magnitude to minimize loss. This occurs because the merge vector must simultaneously accommodate

Table 1: **Summary of task-specific datasets**, with their corresponding sizes and languages.

Task Category	Size	Datasets (Language)
VQA	588K	GQA (en) [34], VQAv2 (en) [29], OKVQA (en) [57], LLaVA-Instruct (zh) [48], CogVLM-Singleround (en&zh) [78], CogVLM-Multiround (en&zh) [78]
Geometry	190K	GeoQA+ (zh) [6], G-LLaVA (en) [23]
Chart	218K	ChartQA (en) [58], DVQA (en) [37]
OCR	238K	OCRVQA (en) [62], TextCaps (en) [67], SynthDoG (en) [40], LLaVAR (en) [96], ST-VQA (en) [5], TextVQA (en) [68], DocVQA (en) [59], DeepForm (en) [72], KLC (en) [69], TabFact (en) [10]
Grounding	135K	RefCOCO (en) [55, 92], VG (en) [41]

multiple task vectors in different directions. Without constraints, Eq. (1) encourages orthogonality by increasing the length of the merge vector (see Fig. 3). When added to the base model, such large-norm task vectors cause deviation from the original distribution, resulting in collapsed language ability [90]. To address this, (i) we adopt SGD instead of Adam, as it better escapes local optima in flat regions and offers greater stability with sparse gradients. (ii) We propose a direct low-rank approximation of  $\tau_{i,l}$  without centering, which helps reduce the Frobenius norm of task vectors. (iii) We also introduce initializing the merged vector with the mean of task vectors to mitigate the issue of excessive merge vector magnitude. As shown in Fig. 4, our approach maintains a relatively consistent norm throughout the optimization process while minimizing loss.

## 5 MLLMs Merging Benchmark

### 5.1 Benchmark Details

**Checkpoint Construction** We select two types of vision-language models representing different scales and usage scenarios: InternVL2.5-1B-Instruct [13], a lightweight aligned model, and Qwen2-VL-7B-Base [77], a general-purpose foundation model. ‘‘Instruct’’ denotes the instruction-following version of a pre-trained model, which is the variant most commonly released. In contrast, Qwen2-VL-Base is one of the few publicly available pre-trained model versions. For InternVL2.5-1B-Instruct, we perform full fine-tuning with a learning rate of 4e-5 and a warmup ratio of 3e-2. For Qwen2-VL-7B-Base, we apply LoRA fine-tuning with a rank of 8, a learning rate of 1e-5, and a warmup ratio of 1e-1. Both models are trained for one epoch using a cosine learning rate scheduler. Different training strategies and scales help evaluate the generalizability of merging methods.

For modality merging, we follow prior work [7] and select Vicuna-7B-v1.5 [97] as the shared LLM. The vision-language model uses CLIP-ViT-L-336px [66] as the image encoder, paired with an MLP projection as the connector. The audio-language model adopts BEATs-Iter3+ [9] as the audio encoder, with a Q-Former incorporating 32 query tokens as the connector. The video-language model employs LanguageBind [98] as the video encoder, also using an MLP connector. See App. D for details.

**Training Data** Following [13], we collect a broader range of domain-specific data, divided into VQA, Geometry, Chart, OCR, and Grounding tasks. The datasets used are summarized in Table 1. For effective supervised fine-tuning, we gather at least 100k public dataset samples for each task, ensuring maximum diversity wherever possible. We process all data into the instruction tuning format. Specifically, for grounding tasks, we map coordinates to the [0,1000) range and add the special token notation <|box\_start|><|box\_end|> [77]. During Qwen2-VL-Base fine-tuning, we observe that Chinese datasets consistently degraded performance, possibly due to lower data quality or because evaluation benchmarks are primarily in English. Consequently, we use only English datasets for instruction tuning of Qwen2-VL-Base. InternVL2.5-Instruct, already possessing multilingual instruction-following capabilities, is fine-tuned using all available data.

**Evaluation Benchmark** Current benchmarks [8, 22, 42, 50] predominantly evaluate a model’s overall performance but provide limited insights into specific capabilities. Therefore, we carefully select specialized datasets to evaluate distinct abilities across tasks. **(i) For VQA**, we utilize VizWiz [30] and GQA [34] to assess general visual question answering proficiency. **(ii) For Geometry**, we incorporate multiple challenging subsets: ‘‘geometry reasoning’’, ‘‘algebraic reasoning’’ and ‘‘geometry problem solving’’ from MathVista [51], complemented by ‘‘metric geometry - angle’’, ‘‘metric geometry - area’’, ‘‘metric geometry - length’’ and ‘‘solid geometry’’ from MATH-Vision [76]. **(iii)**

Table 2: **Capability merging results on InternVL2.5 (full fine-tuning) across multiple tasks.** For the merging methods, we highlight the best score in bold and the second-best score with underlining.

Methods	VQA		Geometry		Chart		OCR		Grounding			Avg.
	VizWiz GQA (test)	MathVista (mini)	MATH-Vision (mini)	ChartQA (test)	TextVQA (val)	OCRVQA (test)	RefCOCO	RefCOCO+	RefCOCOg			
InternVL2.5-Instruct	29.15	54.62	46.80	18.42	69.48	72.51	41.08	71.69	65.41	67.40	53.66	
Individual VQA	30.58	60.91	35.50	17.11	48.76	63.68	36.04	-	-	-	41.80	
Individual Geometry	13.45	32.80	55.20	25.00	51.76	56.91	35.35	24.73	19.61	23.84	33.86	
Individual Chart	20.16	40.39	23.84	10.53	69.52	54.36	34.83	-	-	-	36.23	
Individual OCR	12.40	22.22	23.31	10.53	36.88	73.00	54.79	73.65	68.01	69.10	44.39	
Individual Grounding	19.09	25.88	28.91	14.47	41.32	58.39	74.87	76.67	71.35	70.09	48.10	
Weight Average [82]	29.96	54.89	49.60	18.42	71.64	74.54	41.86	52.62	45.29	52.39	49.12	
Task Arithmetic [35]	30.67	56.34	45.36	21.05	<u>72.88</u>	76.26	43.39	74.90	68.15	72.75	56.18	
TIES Merging [84]	30.63	56.48	44.50	23.68	72.28	<u>76.29</u>	44.01	<u>76.01</u>	68.45	73.65	56.70	
TA w/ DARE [93]	30.61	56.48	48.45	21.05	<b>73.08</b>	<u>76.30</u>	43.03	74.94	68.07	73.02	56.50	
TIES w/ DARE [93]	30.65	56.11	43.85	<u>27.63</u>	72.72	76.19	43.33	75.10	68.48	73.55	56.76	
TSV Merging [24]	<b>31.15</b>	56.67	52.45	<b>28.95</b>	70.56	75.66	45.38	65.19	58.51	59.17	54.37	
Iso-C [56]	28.21	55.36	48.96	21.05	70.56	69.34	<b>46.51</b>	72.72	66.56	68.50	54.78	
WUDI Merging [14]	<u>31.02</u>	<b>56.96</b>	<u>53.03</u>	17.11	69.19	75.95	46.12	<b>76.06</b>	<b>70.14</b>	<b>74.48</b>	<b>57.00</b>	
WUDI v2 (Ours)	30.97	<b>57.13</b>	<b>54.48</b>	21.05	68.72	76.01	<u>46.35</u>	75.97	<u>69.72</u>	<u>73.94</u>	<b>57.44</b>	
Mixture Training	29.79	61.33	52.83	23.68	70.32	72.96	60.25	72.06	65.93	67.46	57.66	

Table 3: **Capability merging results on Qwen2-VL (LoRA fine-tuning) across multiple tasks.** For the merging methods, we highlight the best score in bold and the second-best score with underlining.

Methods	VQA		Geometry		Chart		OCR		Grounding			Avg.
	VizWiz GQA (test)	MathVista (mini)	MATH-Vision (mini)	ChartQA (test)	TextVQA (val)	OCRVQA (test)	RefCOCO	RefCOCO+	RefCOCOg			
Qwen2-VL-Base	5.52	5.39	47.85	23.68	0.36	20.22	1.07	45.32	37.55	31.26	21.82	
Individual VQA	41.38	62.60	33.71	28.94	66.56	80.21	55.33	39.31	32.71	38.01	47.88	
Individual Geometry	35.57	44.63	42.50	28.95	14.56	73.95	45.96	5.57	2.31	3.90	29.79	
Individual Chart	38.58	24.24	49.28	32.89	61.08	79.75	63.67	46.28	36.67	34.06	46.65	
Individual OCR	28.38	37.53	31.81	13.16	57.40	70.50	64.68	0.59	0.46	0.26	30.48	
Individual Grounding	38.60	32.92	36.17	19.74	18.08	75.05	48.27	72.14	65.33	66.48	47.28	
Weight Average [82]	41.47	57.33	<u>50.21</u>	34.21	59.56	81.09	57.85	80.72	65.37	77.68	60.55	
Task Arithmetic [35]	40.52	<b>62.31</b>	40.36	26.31	<u>79.67</u>	81.09	59.50	75.96	61.33	75.85	60.29	
TIES Merging [84]	41.38	59.08	46.87	34.21	67.24	81.42	58.53	80.63	65.36	77.65	61.24	
TA w/ DARE [93]	40.64	<b>62.38</b>	40.67	26.31	<b>79.76</b>	81.04	59.34	75.83	61.41	75.80	60.32	
TIES w/ DARE [93]	<b>41.63</b>	59.96	45.72	<u>35.53</u>	70.68	<u>81.53</u>	59.63	<u>80.73</u>	<b>65.65</b>	<u>77.77</u>	<b>61.88</b>	
TSV Merging [24]	41.43	57.31	<b>51.05</b>	34.21	59.44	81.25	57.81	80.71	65.34	77.76	60.63	
Iso-C [56]	12.31	13.44	39.96	27.63	2.80	30.05	6.12	53.68	38.96	41.90	26.69	
WUDI Merging [14]	37.19	56.45	42.96	27.63	67.84	79.92	<b>65.56</b>	76.25	60.72	71.99	58.65	
WUDI v2 (Ours)	<b>41.61</b>	61.16	48.66	<b>40.79</b>	74.08	<b>81.54</b>	<u>60.06</u>	<b>80.92</b>	<b>65.90</b>	<b>78.24</b>	<b>63.30</b>	
Qwen2-VL-Instruct	44.09	62.18	46.02	19.73	70.04	78.38	65.42	82.89	77.87	75.63	62.23	

**For Chart**, we employ ChartQA [58], which tests reasoning and interpretation ability with charts and graphs. **(iv) For OCR**, our evaluation suite includes TextVQA [68] and OCRVQA [62]. **(v) For Grounding**, we implement referring expression comprehension using RefCOCO [38], RefCOCO+ [38], and RefCOCOg [55], which require models to identify specific objects in images based on natural language descriptions. All evaluation results are obtained using the VLMEvalKit [20] and LMMs-Eval [95] libraries under the same settings to ensure fair comparison. When evaluating MathVista and MATH-Vision benchmarks, we utilize the GPT-4o-mini API to extract answers from the output. All experiments are conducted using 8 NVIDIA V100 GPUs.

For Omni-language models, we select audio-visual question answering task, which involves answering questions about visual objects, sounds, and their relationships in videos. This task requires multimodal understanding and spatio-temporal reasoning over audio-visual scenes. AVQA [89] targets real-world objects and activities. MUSIC-AVQA [44] specifically focuses on musical performances.

## 5.2 Merging Details

Following Task Arithmetic [35], we employ a single coefficient  $\lambda$  to scale the merged vector before adding it to the base model. For all model merging methods, we determine the optimal merging coefficient  $\lambda$  by searching within the range [0.1, 0.3, 0.5, 0.7, 1.0, 1.5]. In our implementation, we use the Adam optimizer with a learning rate of 1e-5 for InternVL while applying the SGD optimizer with a learning rate of 1e-4 for QwenVL. The number of optimization iterations is set to 300. Consistent with prior work [14], we apply our method exclusively to the linear layer in the model.

## 5.3 Experimental Results

**Individual models.** As shown in Table 2 and Table 3, models obtained through SFT demonstrate improvements across their respective tasks. Notably, Qwen2-VL-Base, which initially lacks instruction-following capabilities, learns the correct response format after SFT. For the already

Table 4: **Modality merging results on zero-shot image-audio-video question answering tasks** by merging vision-language, audio-language, and video-language models. The “Individual Modalities” columns show baseline performance for each single-modality model.

Datasets	Individual Modalities			Merging Methods						Online Composing		
	Vision	Audio	Video	Weight Average [82]	Task Arithmetic [35]	Ties Merging [84]	TSV Merging [24]	Iso-C Merging [56]	WUDI Merging [14]	WUDI v2 (Ours)	NaiveMC [7]	DAMC [7]
MUSIC-AVQA	50.77	27.93	49.02	47.75	52.14	50.35	<b>53.78</b>	52.77	52.43	<u>53.17</u>	53.50	52.80
AVQA	75.55	47.57	79.20	69.39	78.62	75.84	<b>80.90</b>	77.51	76.86	<u>80.82</u>	80.26	80.78
Avg.	63.16	37.75	64.11	58.57	65.38	63.10	<b>67.34</b>	65.14	64.65	<u>67.00</u>	66.88	66.79

comprehensive InternVL2.5-Instruct model, individual models enhance specific capabilities but sacrifice generalization performance [25, 94]. We observe that OCR and Grounding tasks exhibit complementary benefits, indicating task similarity. In the table, the “-” indicates instances where the model failed to output in the correct grounding format, *i.e.*, normalized coordinate boxes.

**Capability merging.** Task vectors from individual models effectively capture specialized capabilities, enabling successful model merging. By combining these strengths, model merging outperforms expert MLLMs in their respective tasks. For example, the merged Qwen2-VL significantly outperforms individual models on Geometry task (51.05 and 40.79 vs. 42.50 and 28.95) and Chart task (79.76 vs. 61.08). Similar improvements are also observed for OCR and Grounding tasks. For InternVL2.5-Instruct, we conduct mixture training by combining all task-specific training data for SFT. For Qwen2-VL-Base, we directly use Qwen2-VL-Instruct as the upper bound for mixture training, given its extensive prior SFT with diverse datasets. Notably, our best model merging methods closely match or even surpass mixture training and instruct versions. These results demonstrate that model merging potentially surpasses multi-task learning while providing a scalable solution for creating high-performing MLLMs with reduced computational cost and time.

**Categorization of merging methods.** Different model merging methods demonstrate distinct characteristics. Linear interpolation of task vectors, while neglecting parameter conflicts, achieves robust yet only moderate performance. Sparsification-based methods assume that pruning redundant parameters improves outcomes. TIES struggles to control sparsity levels, often underperforming compared to task arithmetic. DARE consistently delivers plug-and-play improvements through rescaling operations that approximate the original embedding. SVD-based methods’ performance correlates with task vectors’ spectral properties. For example, Iso-C fails on Qwen2-VL because the LoRA-tuned task vectors are already low-rank, and averaging singular values further reduces their Frobenius norm, creating instability in LLMs. Even increasing  $\lambda$ , as recommended in their paper, only marginally improves results. TSV merging excels in modality merging because its orthogonalization mitigates modal conflicts, but delivers ordinary performance in multi-task settings. In contrast, our approach achieves superior average results across various scenarios, benefiting from more accurate task vector estimation and more stable optimization.

**Modality merging.** As shown in Table 4, merging methods effectively integrate information from three modalities, outperforming models trained on individual vision, audio, or video inputs. This highlights the complementary nature of modal information and its potential for merging. Online composing dynamically merges activations in the LLM from different modalities during inference, requiring separate parameter storage for each modality (*i.e.*,  $3 \times$  static merging). NaiveMC [7] performs simple activation averaging, while DAMC [7] decouples parameters during training to reduce modal interference. Notably, the best merging method even outperforms these online composition methods. Advancing Omni models through model merging offers a promising direction for future research.

**Improved task vector optimization.** Our method enhances task vector optimization stability, achieving optimal results. In Table 5, we evaluate each component’s contribution to overall performance. Starting with WUDI merging, we incrementally add one component at a time, reporting performance for both PEFT model merging (Qwen2-VL) and modality merging (Vicuna-7B). Replacing Adam with

Table 5: **The ablation study.**

	Qwen2-VL	Vicuna-7B
WUDI Merging	58.65	64.65
+ SGD	48.88( <b>-9.77%</b> )	66.91( <b>+2.26%</b> )
+ Initialization	63.08( <b>+4.43%</b> )	<b>67.07</b> ( <b>+2.42%</b> )
+ Low-rank	<b>63.30</b> ( <b>+4.65%</b> )	67.00( <b>+2.35%</b> )

Table 7: Merging results on actual fine-tuned checkpoints collected from Hugging Face.

Methods	VQA		Geometry		Chart		OCR		Grounding			Avg.
	VizWiz GQA (test)	MathVista (mini)	MATH-Vision (mini)	ChartQA (test)	TextVQA (val)	OCRVQA (test)	RefCOCO	RefCOCO+	RefCOCOg			
Qwen2-VL-7B-GRPO-8k	44.13	62.04	46.74	22.37	69.20	78.58	68.85	84.13	79.12	76.54	63.17	
Qwen2-VL-7B-Pokemon	42.51	60.96	43.69	19.74	63.20	76.75	67.64	70.11	68.80	68.64	58.20	
olmOCR-7B-0225-preview	43.76	61.48	38.91	18.42	67.48	77.24	68.29	75.17	71.55	69.64	59.19	
EraX-VL-7B-V1.0	36.09	54.36	38.58	25.00	56.00	70.70	65.59	41.89	40.99	43.26	47.25	
Weight Average [82]	43.74	61.30	43.96	26.63	76.40	82.11	71.61	89.54	82.18	86.43	66.39	
Task Arithmetic [35]	41.57	60.95	42.99	23.68	75.28	81.95	71.78	87.72	81.60	85.63	65.32	
TIES Merging [84]	44.17	60.54	42.52	<b>27.95</b>	75.48	82.40	71.09	<b>90.06</b>	<b>83.52</b>	86.44	66.42	
TA w/ DARE [93]	43.33	61.15	<b>44.37</b>	26.95	<b>76.48</b>	82.93	<b>72.00</b>	88.93	82.79	86.07	66.50	
TIES w/ DARE [93]	<b>44.37</b>	60.78	<b>44.37</b>	27.63	76.04	82.61	70.93	89.40	82.93	<b>86.77</b>	<b>66.58</b>	
TSV Merging [24]	43.73	<b>61.40</b>	43.54	27.94	76.44	83.15	71.65	88.53	82.25	86.41	66.50	
Iso-C [36]	43.99	<b>61.34</b>	40.91	22.37	<b>76.96</b>	<b>83.33</b>	71.55	87.74	82.10	85.27	65.56	
WUDI Merging [14]	41.39	60.11	44.20	21.05	74.36	80.78	71.12	87.96	81.50	85.48	64.80	
WUDI v2 (Ours)	43.76	61.29	<b>44.68</b>	27.63	76.24	82.97	71.48	<b>89.56</b>	<b>82.97</b>	86.42	<b>66.70</b>	
Qwen2-VL-Instruct	44.09	62.18	46.02	19.73	70.04	78.38	65.42	82.89	77.87	75.63	[62.23]	

SGD alone does not necessarily improve performance; however, when combined with initializing the merged vector using the mean of task vectors, we observe a significant 4.43% improvement. Low-rank approximation further enhances performance, demonstrating its effectiveness in preserving critical knowledge from task vectors while maintaining the stability of the Frobenius norm.

**Computational requirements.** As illustrated in Table 6, we compare the solving time and GPU memory usage of our approach against mixture training. Our approach optimizes the merged vector over 300 iterations while incurring minimal computational overhead and requiring significantly less GPU memory than data-based training. This efficiency is achieved through layer-by-layer optimization without requiring training data. Our results confirm that the proposed method is computationally efficient and highly scalable on devices with modern GPUs, facilitating the rapid development of new models based on existing ones.

Table 6: Model merging vs. Data mixing.

Methods	Solving Time	GPU Memory
InternVL2.5-1B (Ours)	0.22h	2.62GB
InternVL2.5-1B (Mixed)	25.38h	240GB
Qwen2-VL-7B (Ours)	3.78h	21.97GB
Qwen2-VL-7B (Mixed)	24.56h	256GB

**Actual checkpoints from Hugging Face.** To evaluate the practicality of model merging in communities, we collect fine-tuned models released by different developers on Hugging Face. Our collection includes a model specialized in math reasoning via multimodal reinforcement learning<sup>1</sup>, a personalized model for the Pokemon domain<sup>2</sup>, a model focused on converting PDF documents into text<sup>3</sup>, and a model with OCR and VQA capabilities in Vietnamese<sup>4</sup>. As shown in Table 7, various merging methods achieve performance that surpasses that of the individual models. These results demonstrate that model merging can effectively integrate knowledge from diverse models to construct a more robust system, underscoring its promising practical applications.

## 6 Limitation and Future Work

Due to resource constraints, our experiments were limited to models of 7B parameters. The public datasets we collected may contain lower-quality data that hasn’t undergone rigorous cleaning. Future work will explore multilingual or reasoning-focused MLLM merging, incorporating visual chain-of-thought datasets [46, 91] to support expert reasoning models. For evaluation, we plan to develop new benchmarks specifically designed to assess the reasoning capabilities of MLLMs.

## 7 Conclusion

Model merging aims to combine multiple expert models into a single model without requiring data. In this paper, we introduce the model merging benchmark with detailed categorization of MLLM capabilities, and explore how model merging can effectively combine different modalities of MLLMs. We further propose a novel merging method that effectively removes noise from task vectors and

<sup>1</sup><https://huggingface.co/lmms-lab/Qwen2-VL-7B-GRPO-8k>

<sup>2</sup><https://huggingface.co/hiyouga/Qwen2-VL-7B-Pokemon>

<sup>3</sup><https://huggingface.co/allenai/olmOCR-7B-0225-preview>

<sup>4</sup><https://huggingface.co/erax-ai/EraX-VL-7B-V1.0>

improves the robustness of merged vector optimization. Our results demonstrate that model merging potentially surpasses mixture training, serving as a way for omni model alignment, while offering a scalable solution for developing MLLMs with reduced computational cost and time.

## Acknowledgments

We would like to thank Chi Chen and Shixin Jiang for their assistance in collecting datasets related to modality merging. We are also grateful to the Qwen Team, OpenGVLab, and the developers of the open-source models used in this work for their generous contributions. Additionally, we thank the creators of VLMEvalKit and LMMs-Eval for providing essential evaluation tools.

## References

- [1] Hervé Abdi and Lynne J Williams. Principal component analysis. *Wiley interdisciplinary reviews: computational statistics*, 2010. 5
- [2] Josh Achiam, Steven Adler, Sandhini Agarwal, Lama Ahmad, Ilge Akkaya, Florencia Leoni Aleman, Diogo Almeida, Janko Altenschmidt, Sam Altman, Shyamal Anadkat, et al. GPT-4 technical report. *arXiv preprint arXiv:2303.08774*, 2023. 19
- [3] Arash Ahmadian, Seraphina Goldfarb-Tarrant, Beyza Ermis, Marzieh Fadaee, Sara Hooker, et al. Mix data or merge models? optimizing for diverse multi-task learning. *arXiv preprint arXiv:2410.10801*, 2024. 2
- [4] Takuya Akiba, Makoto Shing, Yujin Tang, Qi Sun, and David Ha. Evolutionary optimization of model merging recipes. *Nature Machine Intelligence*, 2025. 1
- [5] Ali Furkan Biten, Ruben Tito, Andres Mafla, Lluis Gomez, Marçal Rusinol, Ernest Valveny, CV Jawahar, and Dimosthenis Karatzas. Scene text visual question answering. In *ICCV*, 2019. 6
- [6] Jie Cao and Jing Xiao. An augmented benchmark dataset for geometric question answering through dual parallel text encoding. In *COLING*, 2022. 6
- [7] Chi Chen, Yiyang Du, Zheng Fang, Ziyue Wang, Fuwen Luo, Peng Li, Ming Yan, Ji Zhang, Fei Huang, Maosong Sun, et al. Model composition for multimodal large language models. In *ACL*, 2024. 3, 6, 8, 19
- [8] Lin Chen, Jinsong Li, Xiaoyi Dong, Pan Zhang, Yuhang Zang, Zehui Chen, Haodong Duan, Jiaqi Wang, Yu Qiao, Dahua Lin, and Feng Zhao. Are we on the right way for evaluating large vision-language models? In *NeurIPS*, 2024. 6
- [9] Sanyuan Chen, Yu Wu, Chengyi Wang, Shujie Liu, Daniel Tompkins, Zhuo Chen, Wanxiang Che, Xiangzhan Yu, and Furu Wei. BEATs: Audio pre-training with acoustic tokenizers. In *ICML*, 2023. 6, 19
- [10] Wenhui Chen, Hongmin Wang, Jianshu Chen, Yunkai Zhang, Hong Wang, Shiyang Li, Xiyou Zhou, and William Yang Wang. TabFact: A large-scale dataset for table-based fact verification. *arXiv preprint arXiv:1909.02164*, 2019. 6
- [11] Yan-Lun Chen, Yi-Ru Wei, Chia-Yi Hsu, Chia-Mu Yu, Chun-Ying Huang, Ying-Dar Lin, Yu-Sung Wu, and Wei-Bin Lee. Layer-aware task arithmetic: Disentangling task-specific and instruction-following knowledge. *arXiv preprint arXiv:2502.20186*, 2025. 3
- [12] Zhuokun Chen, Jinwu Hu, Zeshuai Deng, Yufeng Wang, Bohan Zhuang, and Mingkui Tan. Enhancing perception capabilities of multimodal llms with training-free fusion. *arXiv preprint arXiv:2412.01289*, 2024. 3
- [13] Zhe Chen, Weiyun Wang, Yue Cao, Yangzhou Liu, Zhangwei Gao, Erfei Cui, Jinguo Zhu, Shenglong Ye, Hao Tian, Zhaoyang Liu, et al. Expanding performance boundaries of open-source multimodal models with model, data, and test-time scaling. *arXiv preprint arXiv:2412.05271*, 2024. 6
- [14] Runxi Cheng, Feng Xiong, Yongxian Wei, Wanyun Zhu, and Chun Yuan. Whoever started the interference should end it: Guiding data-free model merging via task vectors. In *ICML*, 2025. 3, 4, 7, 8, 9, 19
- [15] Jiho Choi, Donggyun Kim, Chanhyuk Lee, and Seunghoon Hong. Revisiting weight averaging for model merging. *arXiv preprint arXiv:2412.12153*, 2024. 3, 5
- [16] Hyung Won Chung, Le Hou, Shayne Longpre, Barret Zoph, Yi Tay, William Fedus, Yunxuan Li, Xuezhi Wang, Mostafa Dehghani, Siddhartha Brahma, et al. Scaling instruction-finetuned language models. *JMLR*, 2024. 4
- [17] Nico Daheim, Thomas Möllenhoff, Edoardo Ponti, Iryna Gurevych, and Mohammad Emtiyaz Khan. Model merging by uncertainty-based gradient matching. In *ICLR*, 2024. 3
- [18] Wenliang Dai, Junnan Li, Dongxu Li, Anthony Tiong, Junqi Zhao, Weisheng Wang, Boyang Li, Pascale Fung, and Steven Hoi. InstructBLIP: Towards general-purpose vision-language models with instruction tuning. In *NeurIPS*, 2023. 18
- [19] Yiyang Du, Xiaochen Wang, Chi Chen, Jiabo Ye, Yiru Wang, Peng Li, Ming Yan, Ji Zhang, Fei Huang, Zhifang Sui, et al. AdaMMS: Model merging for heterogeneous multimodal large language models with unsupervised coefficient optimization. In *CVPR*, 2025. 2, 3
- [20] Haodong Duan, Junming Yang, Yuxuan Qiao, Xinyu Fang, Lin Chen, Yuan Liu, Xiaoyi Dong, Yuhang Zang, Pan Zhang, Jiaqi Wang, et al. VLMEvalKit: An open-source toolkit for evaluating large multi-modality models. In *MM*, 2024. 7
- [21] Junfeng Fang, Houcheng Jiang, Kun Wang, Yunshan Ma, Xiang Wang, Xiangnan He, and Tat-seng Chua. Alphaedit: Null-space constrained knowledge editing for language models. In *ICLR*, 2025. 1

[22] Chaoyou Fu, Peixian Chen, Yunhang Shen, Yulei Qin, Mengdan Zhang, Xu Lin, Jinrui Yang, Xiawu Zheng, Ke Li, Xing Sun, et al. MME: A comprehensive evaluation benchmark for multimodal large language models. *arXiv preprint arXiv:2306.13394*, 2024. 6, 18

[23] Jiahui Gao, Renjie Pi, Jipeng Zhang, Jiacheng Ye, Wanjun Zhong, Yufei Wang, Lanqing Hong, Jianhua Han, Hang Xu, Zhenguo Li, et al. G-LLaVA: Solving geometric problem with multi-modal large language model. *arXiv preprint arXiv:2312.11370*, 2023. 6

[24] Antonio Andrea Gargiulo, Donato Crisostomi, Maria Sofia Bucarelli, Simone Scardapane, Fabrizio Silvestri, and Emanuele Rodolà. Task singular vectors: Reducing task interference in model merging. In *CVPR*, 2025. 3, 4, 7, 8, 9

[25] Sreyan Ghosh, Chandra Kiran Reddy Evuru, Sonal Kumar, S Ramaseswaran, Deepali Aneja, Zeyu Jin, Ramani Duraiswami, and Dinesh Manocha. A closer look at the limitations of instruction tuning. In *ICML*, 2024. 8

[26] Charles Goddard, Shamane Siriwardhana, Malikeh Ehghaghi, Luke Meyers, Vladimir Karpukhin, Brian Benedict, Mark McQuade, and Jacob Solawetz. Arcee’s mergekit: A toolkit for merging large language models. In *EMNLP*, 2024. 3

[27] Yuan Gong, Hongyin Luo, Alexander H. Liu, Leonid Karlinsky, and James R. Glass. Listen, think, and understand. In *ICLR*, 2024. 19

[28] Robert Mansel Gower, Nicolas Loizou, Xun Qian, Alibek Sailanbayev, Egor Shulgin, and Peter Richtárik. SGD: General analysis and improved rates. In *ICML*, 2019. 16

[29] Yash Goyal, Tejas Khot, Douglas Summers-Stay, Dhruv Batra, and Devi Parikh. Making the v in vqa matter: Elevating the role of image understanding in visual question answering. In *CVPR*, 2017. 6

[30] Danna Gurari, Qing Li, Abigale J Stangl, Anhong Guo, Chi Lin, Kristen Grauman, Jiebo Luo, and Jeffrey P Bigham. VizWiz grand challenge: Answering visual questions from blind people. In *CVPR*, 2018. 6

[31] Yifei He, Yuzheng Hu, Yong Lin, Tong Zhang, and Han Zhao. Localize-and-stitch: Efficient model merging via sparse task arithmetic. *TMLR*, 2025. 3

[32] Chenyu Huang, Peng Ye, Tao Chen, Tong He, Xiangyu Yue, and Wanli Ouyang. EMR-Merging: Tuning-free high-performance model merging. In *NeurIPS*, 2024. 3

[33] Wenke Huang, Jian Liang, Xianda Guo, Yiyang Fang, Guancheng Wan, Xuankun Rong, Chi Wen, Zekun Shi, Qingyun Li, Didi Zhu, et al. Keeping yourself is important in downstream tuning multimodal large language model. *arXiv preprint arXiv:2503.04543*, 2025. 19

[34] Drew A Hudson and Christopher D Manning. GQA: A new dataset for real-world visual reasoning and compositional question answering. In *CVPR*, 2019. 6

[35] Gabriel Ilharco, Marco Tulio Ribeiro, Mitchell Wortsman, Ludwig Schmidt, Hannaneh Hajishirzi, and Ali Farhadi. Editing models with task arithmetic. In *ICLR*, 2023. 1, 3, 4, 7, 8, 9, 17

[36] Shixin Jiang, Jiafeng Liang, Ming Liu, and Bing Qin. From specific-mllm to omni-mllm: A survey about the mllms alligned with multi-modality. *arXiv preprint arXiv:2412.11694*, 2024. 2

[37] Kushal Kafle, Brian Price, Scott Cohen, and Christopher Kanan. DVQA: Understanding data visualizations via question answering. In *CVPR*, 2018. 6

[38] Sahar Kazemzadeh, Vicente Ordonez, Mark Matten, and Tamara Berg. Referitgame: Referring to objects in photographs of natural scenes. In *EMNLP*, 2014. 7

[39] Ahmed Khaled and Peter Richtárik. Better theory for SGD in the nonconvex world. *TMLR*, 2023. 16

[40] Geewook Kim, Teakgyu Hong, Moonbin Yim, JeongYeon Nam, Jinyoung Park, Jinyeong Yim, Wonseok Hwang, Sangdoo Yun, Dongyoon Han, and Seunghyun Park. Ocr-free document understanding transformer. In *ECCV*, 2022. 6

[41] Ranjay Krishna, Yuke Zhu, Oliver Groth, Justin Johnson, Kenji Hata, Joshua Kravitz, Stephanie Chen, Yannis Kalantidis, Li-Jia Li, David A Shamma, et al. Visual genome: Connecting language and vision using crowdsourced dense image annotations. *IJCV*, 2017. 6

[42] Bohao Li, Yuying Ge, Yixiao Ge, Guangzhi Wang, Rui Wang, Ruimao Zhang, and Ying Shan. Seed-bench: Benchmarking multimodal large language models. In *CVPR*, 2024. 6, 18

[43] Bo Li, Yuanhan Zhang, Dong Guo, Renrui Zhang, Feng Li, Hao Zhang, Kaichen Zhang, Peiyuan Zhang, Yanwei Li, Ziwei Liu, and Chunyuan Li. LLaVA-onevision: Easy visual task transfer. *TMLR*, 2025. 2

[44] Guangyao Li, Yake Wei, Yapeng Tian, Chenliang Xu, Ji-Rong Wen, and Di Hu. Learning to answer questions in dynamic audio-visual scenarios. In *CVPR*, 2022. 7

[45] Lu Li, Tianyu Zhang, Zhiqi Bu, Suyuchen Wang, Huan He, Jie Fu, Yonghui Wu, Jiang Bian, Yong Chen, and Yoshua Bengio. MAP: Low-compute model merging with amortized pareto fronts via quadratic approximation. In *ICLR*, 2025. 4

[46] Zhong-Zhi Li, Duzhen Zhang, Ming-Liang Zhang, Jiaxin Zhang, Zengyan Liu, Yuxuan Yao, Haotian Xu, Junhao Zheng, Pei-Jie Wang, Xiuyi Chen, et al. From system 1 to system 2: A survey of reasoning large language models. *arXiv preprint arXiv:2502.17419*, 2025. 9

[47] Bin Lin, Yang Ye, Bin Zhu, Jiaxi Cui, Munan Ning, Peng Jin, and Li Yuan. Video-LLaVA: Learning united visual representation by alignment before projection. In *EMNLP*, 2024. 19

[48] Haotian Liu, Chunyuan Li, Yuheng Li, and Yong Jae Lee. Improved baselines with visual instruction tuning. In *CVPR*, 2024. 2, 3, 6, 19

[49] Haotian Liu, Chunyuan Li, Qingyang Wu, and Yong Jae Lee. Visual instruction tuning. In *NeurIPS*, 2023. 18, 19

[50] Yuan Liu, Haodong Duan, Yuanhan Zhang, Bo Li, Songyang Zhang, Wangbo Zhao, Yike Yuan, Jiaqi Wang, Conghui He, Ziwei Liu, et al. MMBench: Is your multi-modal model an all-around player? In *ECCV*, 2024. 6, 18

[51] Pan Lu, Hritik Bansal, Tony Xia, Jiacheng Liu, Chunyuan Li, Hannaneh Hajishirzi, Hao Cheng, Kai-Wei Chang, Michel Galley, and Jianfeng Gao. MathVista: Evaluating mathematical reasoning of foundation models in visual contexts. In *ICLR*, 2024. 6

[52] Zhenyi Lu, Chenghao Fan, Wei Wei, Xiaoye Qu, Dangyang Chen, and Yu Cheng. Twin-Merging: Dynamic integration of modular expertise in model merging. In *NeurIPS*, 2024. 3

[53] Ruipu Luo, Ziwang Zhao, Min Yang, Junwei Dong, Da Li, Pengcheng Lu, Tao Wang, Linmei Hu, Minghui Qiu, and Zhongyu Wei. Valley: Video assistant with large language model enhanced ability. *arXiv preprint arXiv:2306.07207*, 2023. 19

[54] Muhammad Maaz, Hanoona Rasheed, Salman Khan, and Fahad Khan. Video-ChatGPT: Towards detailed video understanding via large vision and language models. In *ACL*, 2024. 19

[55] Junhua Mao, Jonathan Huang, Alexander Toshev, Oana Camburu, Alan L Yuille, and Kevin Murphy. Generation and comprehension of unambiguous object descriptions. In *CVPR*, 2016. 6, 7

[56] Daniel Marczak, Simone Magistri, Sebastian Cygert, Bartłomiej Twardowski, Andrew D Bagdanov, and Joost van de Weijer. No task left behind: Isotropic model merging with common and task-specific subspaces. In *ICML*, 2025. 3, 4, 7, 8, 9

[57] Kenneth Marino, Mohammad Rastegari, Ali Farhadi, and Roorzbeh Mottaghi. OK-VQA: A visual question answering benchmark requiring external knowledge. In *CVPR*, 2019. 6

[58] Ahmed Masry, Do Xuan Long, Jia Qing Tan, Shafiq Joty, and Enamul Hoque. ChartQA: A benchmark for question answering about charts with visual and logical reasoning. *arXiv preprint arXiv:2203.10244*, 2022. 6, 7

[59] Minesh Mathew, Dimosthenis Karatzas, and CV Jawahar. Docvqa: A dataset for vqa on document images. In *WACV*, 2021. 6

[60] Xinhao Mei, Chutong Meng, Haohe Liu, Qiuqiang Kong, Tom Ko, Chengqi Zhao, Mark D Plumbley, Yuexian Zou, and Wenwu Wang. WavCaps: A chatgpt-assisted weakly-labelled audio captioning dataset for audio-language multimodal research. *TASLP*, 2024. 19

[61] Gabriele Merlin, Vedant Nanda, Ruchit Rawal, and Mariya Toneva. What happens during finetuning of vision transformers: An invariance based investigation. In *CoLLAs*, 2023. 4

[62] Anand Mishra, Shashank Shekhar, Ajeet Kumar Singh, and Anirban Chakraborty. OCRVQA: Visual question answering by reading text in images. In *ICDAR*, 2019. 6, 7

[63] Guillermo Ortiz-Jimenez, Alessandro Favero, and Pascal Frossard. Task arithmetic in the tangent space: Improved editing of pre-trained models. In *NeurIPS*, 2023. 4

[64] Artemis Panagopoulou, Le Xue, Ning Yu, Junnan Li, Dongxu Li, Shafiq Joty, Ran Xu, Silvio Savarese, Caiming Xiong, and Juan Carlos Niebles. X-instructblip: A framework for aligning x-modal instruction-aware representations to llms and emergent cross-modal reasoning. *arXiv preprint arXiv:2311.18799*, 2023. 19

[65] Huaizhi Qu, Xinyu Zhao, Jie Peng, Kwonjoon Lee, Behzad Dariush, and Tianlong Chen. UQ-Merge: Uncertainty guided multimodal large language model merging, 2024. 2, 3

[66] Alec Radford, Jong Wook Kim, Chris Hallacy, Aditya Ramesh, Gabriel Goh, Sandhini Agarwal, Girish Sastry, Amanda Askell, Pamela Mishkin, Jack Clark, et al. Learning transferable visual models from natural language supervision. In *ICML*, 2021. 6, 19

[67] Oleksii Sidorov, Ronghang Hu, Marcus Rohrbach, and Amanpreet Singh. TextCaps: a dataset for image captioning with reading comprehension. In *ECCV*, 2020. 6

[68] Amanpreet Singh, Vivek Natarajan, Meet Shah, Yu Jiang, Xinlei Chen, Dhruv Batra, Devi Parikh, and Marcus Rohrbach. Towards vqa models that can read. In *CVPR*, 2019. 6, 7

[69] Tomasz Stanisławek, Filip Graliński, Anna Wróblewska, Dawid Lipiński, Agnieszka Kaliska, Paulina Rosalska, Bartosz Topolski, and Przemysław Biecek. Kleister: key information extraction datasets involving long documents with complex layouts. In *ICDAR*, 2021. 6

[70] George Stoica, Pratik Ramesh, Boglarka Ecsedi, Leshem Choshen, and Judy Hoffman. Model merging with svd to tie the knots. In *ICLR*, 2025. 3

[71] Yi-Lin Sung, Linjie Li, Kevin Lin, Zhe Gan, Mohit Bansal, and Lijuan Wang. An empirical study of multimodal model merging. In *EMNLP*, 2023. 3

[72] Stacey Svetlichnaya. DeepForm: Understand structured documents at scale, 2020. 6

[73] Anke Tang, Li Shen, Yong Luo, Han Hu, Bo Du, and Dacheng Tao. Fusionbench: A comprehensive benchmark of deep model fusion. *arXiv preprint arXiv:2406.03280*, 2024. 17

[74] Anke Tang, Li Shen, Yong Luo, Nan Yin, Lefei Zhang, and Dacheng Tao. Merging multi-task models via weight-ensembling mixture of experts. In *ICML*, 2024. 3

[75] Anke Tang, Li Shen, Yong Luo, Yibing Zhan, Han Hu, Bo Du, Yixin Chen, and Dacheng Tao. Parameter-efficient multi-task model fusion with partial linearization. In *ICLR*, 2024. 4

[76] Ke Wang, Junting Pan, Weikang Shi, Zimu Lu, Houxing Ren, Aojun Zhou, Mingjie Zhan, and Hongsheng Li. Measuring multimodal mathematical reasoning with math-vision dataset. In *NeurIPS*, 2024. 6

[77] Peng Wang, Shuai Bai, Sinan Tan, Shijie Wang, Zhihao Fan, Jinze Bai, Keqin Chen, Xuejing Liu, Jialin Wang, Wenbin Ge, et al. Qwen2-VL: Enhancing vision-language model’s perception of the world at any resolution. *arXiv preprint arXiv:2409.12191*, 2024. 2, 6

[78] Weihan Wang, Qingsong Lv, Wenmeng Yu, Wenyi Hong, Ji Qi, Yan Wang, Junhui Ji, Zhuoyi Yang, Lei Zhao, Song XiXuan, et al. CogVLM: Visual expert for pretrained language models. In *NeurIPS*, 2024. 6

[79] Yongxian Wei, Zixuan Hu, Li Shen, Zhenyi Wang, Chun Yuan, and Dacheng Tao. Open-vocabulary customization from CLIP via data-free knowledge distillation. In *ICLR*, 2025. 19

[80] Yongxian Wei, Anke Tang, Li Shen, Chun Yuan, and Xiaochun Cao. Modeling multi-task model merging as adaptive projective gradient descent. In *ICML*, 2025. 3

[81] Thomas Wolf, Lysandre Debut, Victor Sanh, Julien Chaumond, Clement Delangue, Anthony Moi, Pierrick Cistac, Tim Rault, Rémi Louf, Morgan Funtowicz, et al. Huggingface’s transformers: State-of-the-art natural language processing. *arXiv preprint arXiv:1910.03771*, 2019. 19

[82] Mitchell Wortsman, Gabriel Ilharco, Samir Ya Gadre, Rebecca Roelofs, Raphael Gontijo-Lopes, Ari S Morcos, Hongseok Namkoong, Ali Farhadi, Yair Carmon, Simon Kornblith, et al. Model soups: averaging weights of multiple fine-tuned models improves accuracy without increasing inference time. In *ICML*, 2022. 3, 7, 8, 9

[83] Chengyue Wu, Teng Wang, Yixiao Ge, Zeyu Lu, Ruisong Zhou, Ying Shan, and Ping Luo.  $\pi$ -tuning: Transferring multimodal foundation models with optimal multi-task interpolation. In *ICML*, 2023. 4

[84] Prateek Yadav, Derek Tam, Leshem Choshen, Colin A Raffel, and Mohit Bansal. TIES-merging: Resolving interference when merging models. *NeurIPS*, 2023. 3, 7, 8, 9

[85] Prateek Yadav, Tu Vu, Jonathan Lai, Alexandra Chronopoulou, Manaal Faruqui, Mohit Bansal, and Tsendsuren Munkhdalai. What matters for model merging at scale? *arXiv preprint arXiv:2410.03617*, 2024. 1, 2

[86] Enneng Yang, Li Shen, Guibing Guo, Xingwei Wang, Xiaochun Cao, Jie Zhang, and Dacheng Tao. Model merging in llms, mllms, and beyond: Methods, theories, applications and opportunities. *arXiv preprint arXiv:2408.07666*, 2024. 1

[87] Enneng Yang, Li Shen, Zhenyi Wang, Guibing Guo, Xiaojun Chen, Xingwei Wang, and Dacheng Tao. Representation surgery for multi-task model merging. In *ICML*, 2024. 3

[88] Enneng Yang, Zhenyi Wang, Li Shen, Shiwei Liu, Guibing Guo, Xingwei Wang, and Dacheng Tao. Adamerging: Adaptive model merging for multi-task learning. In *ICLR*, 2024. 3

[89] Pinci Yang, Xin Wang, Xuguang Duan, Hong Chen, Runze Hou, Cong Jin, and Wenwu Zhu. AVQA: A dataset for audio-visual question answering on videos. In *MM*, 2022. 7

[90] Wanli Yang, Fei Sun, Xinyu Ma, Xun Liu, Dawei Yin, and Xueqi Cheng. The butterfly effect of model editing: Few edits can trigger large language models collapse. In *ACL*, 2024. 6

[91] Yi Yang, Xiaoxuan He, Hongkun Pan, Xiyan Jiang, Yan Deng, Xingtao Yang, Haoyu Lu, Dacheng Yin, Fengyun Rao, Minfeng Zhu, et al. R1-onevision: Advancing generalized multimodal reasoning through cross-modal formalization. *arXiv preprint arXiv:2503.10615*, 2025. 9

[92] Licheng Yu, Patrick Poirson, Shan Yang, Alexander C Berg, and Tamara L Berg. Modeling context in referring expressions. In *ECCV*, 2016. 6

[93] Le Yu, Bowen Yu, Haiyang Yu, Fei Huang, and Yongbin Li. Language models are super mario: Absorbing abilities from homologous models as a free lunch. In *ICML*, 2024. 3, 4, 7, 9

- [94] Yuexiang Zhai, Shengbang Tong, Xiao Li, Mu Cai, Qing Qu, Yong Jae Lee, and Yi Ma. Investigating the catastrophic forgetting in multimodal large language model fine-tuning. In *CPAL*, 2024. <sup>8</sup>
- [95] Kaichen Zhang, Bo Li, Peiyuan Zhang, Fanyi Pu, Joshua Adrian Cahyono, Kairui Hu, Shuai Liu, Yuanhan Zhang, Jingkang Yang, Chunyuan Li, et al. Lmms-eval: Reality check on the evaluation of large multimodal models. *arXiv preprint arXiv:2407.12772*, 2024. <sup>7</sup>
- [96] Yanzhe Zhang, Ruiyi Zhang, Jiuxiang Gu, Yufan Zhou, Nedim Lipka, Diyi Yang, and Tong Sun. LLaVAR: Enhanced visual instruction tuning for text-rich image understanding. *arXiv preprint arXiv:2306.17107*, 2023. <sup>6</sup>
- [97] Lianmin Zheng, Wei-Lin Chiang, Ying Sheng, Siyuan Zhuang, Zhanghao Wu, Yonghao Zhuang, Zi Lin, Zhuohan Li, Dacheng Li, Eric Xing, et al. Judging llm-as-a-judge with mt-bench and chatbot arena. In *NeurIPS*, 2023. <sup>6</sup>
- [98] Bin Zhu, Bin Lin, Munan Ning, Yang Yan, Jiaxi Cui, HongFa Wang, Yatian Pang, Wenhao Jiang, Junwu Zhang, Zongwei Li, et al. LanguageBind: Extending video-language pretraining to n-modality by language-based semantic alignment. *arXiv preprint arXiv:2310.01852*, 2023. <sup>6, 19</sup>

## A Theoretical Proofs

**Assumption A.1** (Lipschitz continuous). The loss function used for task  $i$  is  $\mathcal{C}_i$ -Lipschitz continuous; that is, for any  $\Theta$  and  $\Theta'$ :

$$\|\mathcal{L}_i(\Theta) - \mathcal{L}_i(\Theta')\| \leq \mathcal{C}_i \|\Theta - \Theta'\|. \quad (5)$$

Lipschitz continuity of the loss function represents a standard assumption in optimization theory and is widely employed to derive generalization bounds and conduct stability analysis. Consequently, we adopt this assumption to analyze the effect of the loss function in our work.

**Assumption A.2** (Upper bound of second moment). Denote the stochastic gradient in step  $t$  during the optimization process as  $g_t$ . There exists a constant  $\mathcal{G} > 0$  such that:

$$\mathbb{E} [\|g_t(\Theta)\|^2] \leq \mathcal{G}^2. \quad (6)$$

Assumption A.2 has been formulated in various ways throughout the literature. For convex conditions, [28] proposed the bound  $4\mathcal{C}(\mathcal{L}(\Theta) - \mathcal{L}(\Theta_*)) + 2\sigma^2$ , where  $\Theta_*$  is the global minimizer and  $\sigma^2 \triangleq \mathbb{E} [\|g(\Theta_*)\|^2]$ . Similarly, for non-convex settings, [39] introduced the expected smoothness assumption as  $2A(\mathcal{L}(\Theta) - \mathcal{L}^{\inf}) + B \|\nabla \mathcal{L}(\Theta)\|^2 + C$ , for some  $A, B, C \geq 0$  and  $\forall \Theta \in \mathbb{R}^d$ .

**Lemma A.3** (Upper bound of loss affection). Denote the merged task vector as  $\tau_m = \sum_j \alpha_j \tau_j$ , and the task vector of task  $i$  as  $\tau_i$ . Let  $\mathcal{L}_i$  be the loss for task  $i$ . The difference in loss is bounded by the following:

$$\|\mathcal{L}_i(\boldsymbol{\theta}_0 + \tau_m) - \mathcal{L}_i(\boldsymbol{\theta}_0 + \tau_i)\| \leq \sum_j \Psi_j^i \cdot \|\tau_j\|, \quad (7)$$

where  $\Psi_j^i$  is the coefficient capturing how sensitive task  $i$ 's loss is to parameter updates from task  $j$  defined as:

$$\Psi_j^i = \begin{cases} \mathcal{C}_i \cdot |\alpha_j|, & \text{if } j \neq i \\ \mathcal{C}_i \cdot |1 - \alpha_j|, & \text{if } j = i. \end{cases} \quad (8)$$

*Proof.* Under assumption that each  $\mathcal{L}_i$  is  $\mathcal{C}_i$ -Lipschitz, we have:

$$\|\mathcal{L}_i(\boldsymbol{\theta}_0 + \tau_m) - \mathcal{L}_i(\boldsymbol{\theta}_0 + \tau_i)\| \leq \mathcal{C}_i \cdot \|\tau_m - \tau_i\| \quad (9)$$

$$= \mathcal{C}_i \cdot \left\| \sum_j \alpha_j \tau_j - \tau_i \right\| \quad (10)$$

$$\leq \mathcal{C}_i \cdot \left( \sum_{j \neq i} \alpha_j \cdot \|\tau_j\| + |1 - \alpha_i| \cdot \|\tau_i\| \right). \quad (11)$$

We define the coefficient  $\Psi_j^i$  for task  $i$  as follows:

$$\Psi_j^i = \begin{cases} \mathcal{C}_i \cdot |\alpha_j|, & \text{if } j \neq i \\ \mathcal{C}_i \cdot |1 - \alpha_j|, & \text{if } j = i. \end{cases} \quad (12)$$

Applying Eq. (12) to Eq. (11), we obtain:

$$\|\mathcal{L}_i(\boldsymbol{\theta}_0 + \tau_m) - \mathcal{L}_i(\boldsymbol{\theta}_0 + \tau_i)\| \leq \sum_j \Psi_j^i \cdot \|\tau_j\|. \quad (13)$$

□

**Theorem A.4.** Let  $\theta_0 \in \mathbb{R}^d$  be the initial parameter. For each task  $i$ , after  $T$  gradient steps with constant learning rate  $\eta$ , we denote the task vector as  $\tau_i = \theta_i - \theta_0$ . Considering that most methods can be viewed as extensions of linear combinations of task vectors, let  $\tau_m = \sum_j \alpha_j \tau_j$  denote the merged vector. The loss on task  $i$  is denoted by  $\mathcal{L}_i(\Theta)$ , which is  $\mathcal{C}_i$ -Lipschitz continuous. Assuming a constraint on the second moment of the gradient, then:

$$\|\mathcal{L}_i(\theta_0 + \tau_m) - \mathcal{L}_i(\theta_0 + \tau_i)\| \leq \mathcal{O}(\eta T) \quad (14)$$

This indicates that both the learning rate and iterations influence model merging results.

*Proof.* Considering the process of gradient update:

$$\tau_j = \sum_{t=0}^{T-1} -\eta \cdot g_t(\Theta), \quad (15)$$

we have:

$$\mathbb{E}[\|\tau_j\|^2] = \mathbb{E}[\|\sum_{t=0}^{T-1} -\eta \cdot g_t(\Theta)\|^2] \quad (16)$$

$$= \mathbb{E}[\eta^2 \|\sum_{t=0}^{T-1} g_t(\Theta)\|^2] \quad (17)$$

$$\leq \eta^2 \cdot T \cdot \sum_{t=0}^{T-1} \mathbb{E}[\|g_t(\Theta)\|^2] \quad (18)$$

$$\leq \eta^2 \cdot T^2 \cdot \mathcal{G}^2. \quad (19)$$

Since  $\mathbb{E}[X^2] \geq \mathbb{E}^2[X]$ , we can derive:

$$\mathbb{E}[\|\tau_j\|] \leq \sqrt{\mathbb{E}[\|\tau_j\|^2]} \quad (20)$$

$$= \eta \cdot T \cdot \mathcal{G}. \quad (21)$$

Applying Eq. (20) to Lemma A.3, we obtain:

$$\|\mathcal{L}_i(\theta_0 + \tau_m) - \mathcal{L}_i(\theta_0 + \tau_i)\| \leq \underbrace{(\sum_j \Psi_j^i) \cdot \mathcal{G}}_{\text{coefficient}} \cdot \eta T. \quad (22)$$

Therefore, we can summarize as follows:

$$\|\mathcal{L}_i(\theta_0 + \tau_m) - \mathcal{L}_i(\theta_0 + \tau_i)\| \leq \mathcal{O}(\eta T). \quad (23)$$

□

## B Fine-Tuning Influence on Model Merging

To demonstrate the sensitivity of model merging to task vectors  $\tau_i$  (*i.e.*, parameter changes between fine-tuned models and the base model), we conduct experiments using the standard CLIP-ViT model merging [35], following the fine-tuning setup of FusionBench [73]. The Adam optimizer is employed with a fixed learning rate of 1e-5, running for 4000 training steps with a batch size of 32. Models are saved every 500 iterations and evaluated for accuracy on the test dataset, as illustrated in Fig. 5. Convergence is generally observed around 3000 iterations.

Additionally, we evaluate four classical merging methods at various fine-tuning stages, reporting their average accuracy in Fig. 6. The results indicate that increasing the number of fine-tuning steps does not consistently enhance merging performance. Instead, performance typically improves initially before declining. This finding motivates our derivation of Theorem 3.1, which demonstrates that both the learning rate and the number of iterations affect model merging performance. MLLM training is typically organized by full passes over the data (epochs), rather than discrete iteration steps. Accordingly, we set the number of epochs to 1 and reduce the learning rate to limit parameter changes. This keeps the fine-tuned models close to the base model in parameter space while still yielding improvements on specific tasks.

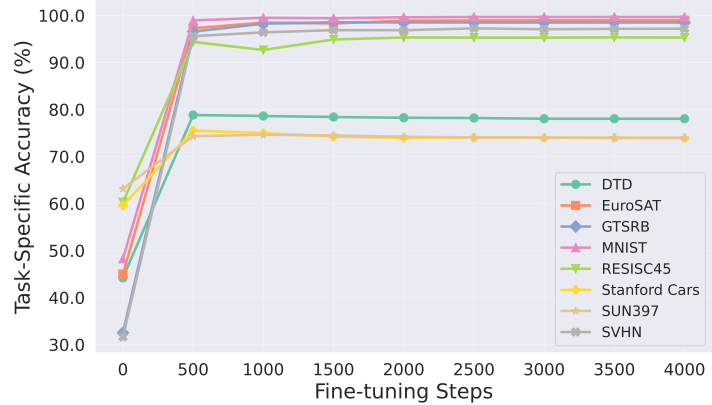


Figure 5: Accuracy of CLIP pre-trained ViT-B/32 fine-tuned separately on eight downstream datasets. As training steps increase, performance on each dataset gradually converges.

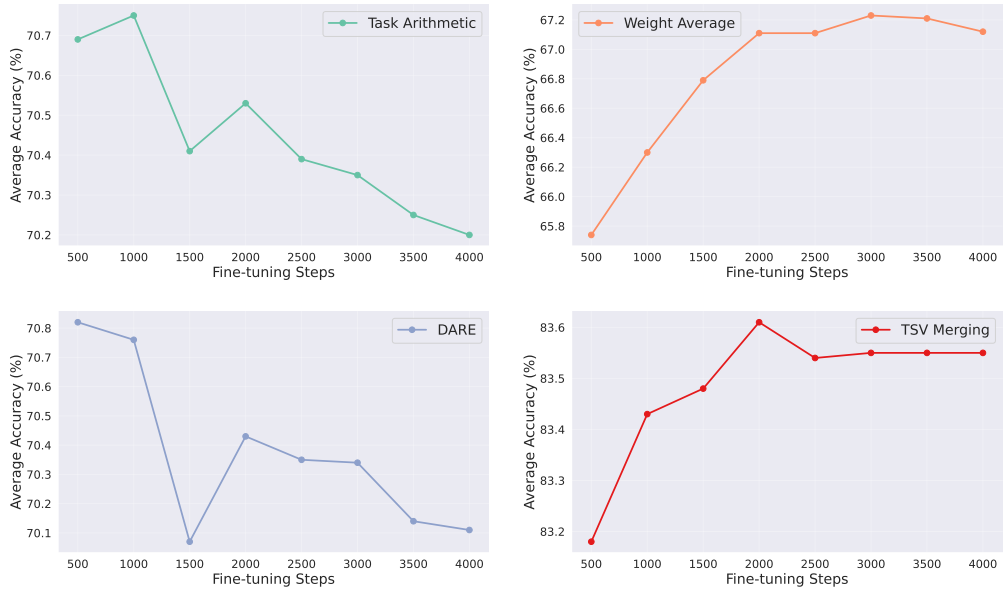


Figure 6: Average accuracy of different model merging methods across eight datasets. Increasing fine-tuning steps does not consistently improve merging performance; instead, performance tends to rise initially and then decline.

## C Challenges of MLLMs Merging Benchmark

**Disconnection between training and evaluation of MLLMs.** Training and evaluation of MLLMs are developed independently rather than being split from the same dataset. (i) Recent benchmarks [22, 42, 50] often assess models’ comprehensive abilities through pre-defined choice questions, with each benchmark emphasizing different nuanced aspects. (ii) Domain-specific training data is also proprietary and confidential. Consequently, models demonstrate varied capabilities based on their training foundations. For example, LLaVA [49] excels in conversational visual reasoning, while InstructBLIP [18] performs better on traditional short-answer VQA tasks. These differences present challenges for developing a unified benchmark suitable for multi-task model merging.

**Trade-off between instruction-following and task-specific capabilities.** Traditional public datasets provide rich visual-specific capabilities but lack instruction-following formats. On the

other hand, instruction-following data generated by models like GPT-4 [2] often lack task-specific characteristics. This creates tension between these two essential aspects of model performance.

**Further SFT may lead to overfitting.** Most publicly available models are already instruction-tuned versions that have undergone extensive training on diverse datasets, including open-source repositories, curated purchased datasets, and private collections. Further SFT often yields diminishing returns, as models may already be overfit to the common datasets used for training [33].

## D Details of Modality Setting

Following DAMC [7], we select modality encoders and connectors paired with Vicuna-7B-v1.5 to train separate models using bi-modal data across three modalities (*i.e.*, vision, audio and video). Additional details are presented in Table 8. The training approach consists of two phases: an alignment stage where only connector parameters are trainable, and a fine-tuning stage where we tune all connector and language model parameters. During fine-tuning, we apply LoRA with a rank of 128 across all linear modules within the LLM. For our merging strategy, we preserve each modality’s unique encoder and connector components while merging only the language model parameters, enabling the model to process inputs from all three modalities simultaneously.

Table 8: Overview of modality components and training data.

Modality	Modality Encoder	Connector	Alignment Data	Fine-tuning Data	Referenced Work
Vision	CLIP-ViT-L-336px [66]	MLP	LCS 558K [49]	LLaVA-mixed 665K [48]	LLaVA-1.5 [48]
Audio	BEATs-Iter3+ [9]	Q-Former	WaveCaps 400K [60]	OpenAQA filtered 350K [27]	X-InstructBLIP [64]
Video	LanguageBind [98]	MLP	LCS 558K [49], Valley 702K [53]	Video-ChatGPT 100K [54], LLaVA-mixed subset 140K [48]	Video-LLaVA [47]

## E Understanding the Task Vector

WUDI Merging [14] substitutes the transpose of the task vector  $\tau_l$  for the input vector  $\mathbf{x}_l$ . We reconsider the update process of the task vector, which can be formulated as follows:

$$\tau_l^k = \sum_{t=1}^T -\eta \cdot \frac{\partial \mathcal{L}(\theta^{t-1})}{\partial \theta_{l,k}^{t-1}} \quad (24)$$

$$= \sum_{t=1}^T -\eta \sum_{n=1}^N \frac{\partial \mathcal{L}(\theta^{t-1})}{\partial (\theta_{l,k}^{t-1} \mathbf{x}_{n,l}^{t-1})} \cdot \frac{\partial (\theta_{l,k}^{t-1} \mathbf{x}_{n,l}^{t-1})}{\partial \theta_{l,k}^{t-1}} \quad (25)$$

$$= \underbrace{\sum_{t=1}^T -\eta \sum_{n=1}^N \frac{\partial \mathcal{L}(\theta^{t-1})}{\partial (\theta_{l,k}^{t-1} \mathbf{x}_{n,l}^{t-1})}}_{\text{coefficient}} \cdot (\mathbf{x}_{n,l}^{t-1})^\top, \quad (26)$$

where  $\tau_l^k$  denotes the task vector of neuron  $k$  in linear layer  $l$ , and  $\theta_{l,k}^{t-1}$  represents the parameters of neuron  $k$  in linear layer  $l$  at time  $t-1$ . Each neuron in the linear layer can be interpreted as a weighted sum of input vectors across training iterations, with gradients serving as coefficients.

## F Broader Impacts

Various developers release fine-tuned models on open-source platforms such as Hugging Face [79, 81]. Model merging reduces storage and serving costs through model reuse and helps preserve data privacy. It also supports decentralized development by enabling independent contributors to train models that can later be merged. We hope this benchmark will help the model merging community better evaluate the generalizability of their methods and accelerate progress in MLLM development.